

## Ultrasonic attenuation changes near the superconducting and melting transition temperatures in a twinned $\text{YBa}_2\text{Cu}_3\text{O}_{7-\delta}$ single crystal

D Dasgupta, J R Feller and Bimal K Sarma\*

Department of Physics, University of Wisconsin-Milwaukee, 1900 E Kenwood Blvd,  
Milwaukee, Wisconsin 53211, USA

E-mail : bksarma@csd.uwm.edu

**Abstract** : Using Sampled Continuous Wave technique and an unique bonding of the sample to the transducer to achieve optimal coupling, quasi free oscillations are set up in a transducer + sample oscillator system using low frequency RF signals. Under optimal coupling conditions, the acoustic energy dissipation is primarily in the crystal and is monitored through the changing Q of the composite oscillator. Ultrasonic experiments performed on a twinned single crystal of  $\text{YBa}_2\text{Cu}_3\text{O}_{7-\delta}$  was able to reveal the superconducting transition in the bulk of the material and also the melting transitions in the flux lattice system in presence of an external magnetic field. The results obtained with this technique, using low frequency and low excitation amplitude, points towards sampled CW technique to be a very sensitive and an alternative experimental probe for small HTS single crystals.

**Keywords** : Ultrasonics, superconductivity, flux lines.

**PACS No.** : 74.60 -w

### 1. Introduction

For over a decade, the high temperature superconducting (HTS) materials are in the focus of intense theoretical and experimental investigations. Much of the interest is in studying the properties of flux lines in the mixed phase of these type-II superconducting materials. A detailed review was done by Blatter *et al* [1]. In most experimental techniques, intrinsic properties of the flux line ensemble are extracted via the interaction of the background ionic lattice with the vortices through pinning. Pankert [2] showed that when the vortex system is sufficiently pinned (*i.e.* below the depinning temperature) ultrasound propagation is influenced by the elastic nature of the flux lines embedded in the sample. Ultrasound induced motion of the ionic lattice interacts with the pinned vortex system to produce dissipation. These ideas were confirmed experimentally [3] for superconductors with high pinning density.

When the flux lines (FLs) are pinned, they are vibrated by ultrasound through the vibration of the pinning centers in the bulk of the sample. Thus all FLs in the sample are vibrated by ultrasound leading to a bulk measurement technique. In contrast, for example, in AC susceptibility measurements, due to shielding of the AC current, only FLs near the surface and the grain boundaries and excited. Also in the long wavelength regime

where the experiments were performed, with  $\lambda \gg$  thickness of the sample, the current density ( $\sim 10^{-4}$  A/cm<sup>2</sup>) due to sound induced ionic motion is orders of magnitude lower than what is usually employed ( $\sim 0.5$  A/cm<sup>2</sup>) in transport experiments and hence this ultrasonic setup mimics the quasi-static state of the FL's more accurately.

A novel ultrasonic technique in the form of sampled CW technique has been found to be ideal for small samples. In this paper we present our results obtained using sampled CW technique on a twinned single crystal of  $\text{YBa}_2\text{Cu}_3\text{O}_{7-\delta}$ . In sampled CW technique, a continuous wave oscillator is gated on for a time  $t_d$  sufficiently long so that steady state conditions in the ultrasonic resonator are achieved. At  $t = t_d$ , the transmitter is gated off, and the receiver which was gated off during the transmitter on portion of the cycle, is gated on. The receiver thus samples the continuous wave ultrasonic signal that was established in the resonator during the transmitter "ON" interval. The output of the transducer, amplified and detected, is proportional to the instantaneous acoustic particle velocity at the  $z = 0$  face of the transducer and is not complicated by the presence of the transmitter voltage. Thus, cross talk is eliminated. The sampled CW technique permits two modes of operation, frequency domain observation and the time domain observation. In the time domain mode of operation, the decay of

\* Corresponding Author

ultrasonic response from the steady state condition is monitored for a fixed frequency  $\omega = \omega_m$ , corresponding to the center of the mechanical resonance of the system.

## 2. Experimental setup

The schematic of the setup for this technique is shown in the bottom part of Figure 1. The  $\text{YBa}_2\text{Cu}_3\text{O}_{7-\delta}$  (YBCO) crystal is placed on an overtone polished and gold plated X-cut quartz transducer. This small crystal is then pressed on to the transducer using very fine threads ( $\sim 1\mu\text{m}$  diameter) of GE-varnish. Thus, there is no "real" bond material used between the transducer and the crystal. The varnish threads were the only means of holding or pressing the sample on to the transducer. It is been theoretically determined that under the optimal coupling condition of  $Q_{\text{sample}} \equiv Q_{\text{transducer}}$  resulting in  $Q_{\text{total}} = \frac{1}{2} * Q_{\text{sample}}$ , the sensitivity is maximum. The transducer is mounted on two long parallel gold wires with both ends fixed, supporting the transducer + sample and also acting as electrical ground connection for the transducer. RF signal is applied to the other side (opposite to that of the gold wires) of the transducer through couple of very soft springs of non magnetic Be-Cu wire, touching the transducer surface as lightly as possible to reduce mechanical load on the transducer + sample system. Thus, the system is designed to oscillate as freely as possible.

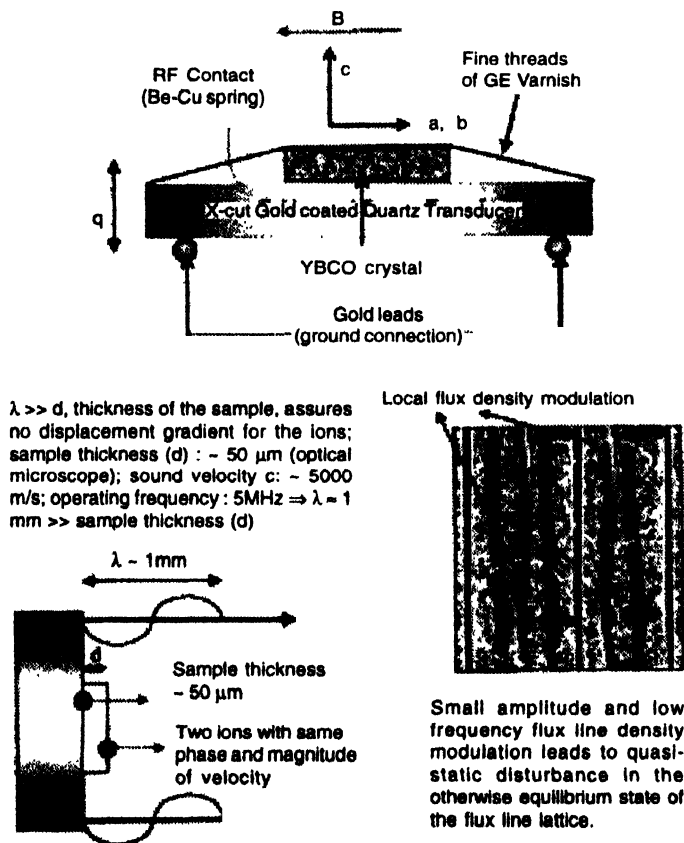


Figure 1. Schematic of experimental setup in sampled CW technique (top) and how ultrasound modulates local FL density (bottom) in a HTS sample.

The probe was cooled with liquid nitrogen in a bath cryostat (Janis Research) and temperature control was done using a Lakeshore Cryotronics temperature controller (DRC93CA) and a carbon-glass resistor temperature sensor. A conventional electromagnet (Varian Fieldial Mark IV) was used to do measurements in magnetic fields up to 1.6 Tesla. RF pulse is generated and detected by a standalone ultrasonic pulse generator and detector unit, RAM-10000, manufactured by RITEC Inc, Warrickshire, RI.

A 5 MHz RF pulse of width 100-150  $\mu\text{s}$  was applied to the transducer, with a repetition rate of 25Hz, setting the transducer + sample oscillator system into mechanical vibration. Immediately after the pulse, the amplitude of oscillation of the system decayed with a characteristic time constant. The attenuation of the oscillator was determined by observing the amplitude of the exponentially decaying profile of the applied RF signal. For this, two high impedance receivers (fast gated boxcar built in to the RAM-10000 system) were used to two known and fixed times after the pulse. With the available electronics, attenuation could easily be determined with a resolution of  $10^{-5}$  dB/ $\mu\text{s}$  or about  $2 \times 10^{-5}$  dB/cm (sound velocity  $\sim 5000$  m/s).

## 3. Experimental results

Experiment was performed on a twinned single crystal of YBCO. The crystal was grown using self-flux technique and has a  $T_c \sim 93.8\text{K}$  with a transition width of  $\sim 0.3\text{K}$  as determined by low field ac-susceptibility experiment. It has dimension of  $1.3 \times 0.75 \times 0.1 \text{ mm}^3$ . Figure 2 shows the changes in sound attenuation as a function of temperature at different magnetic fields applied parallel to the a-b plane of the crystal. The attenuation is obtained after subtracting a constant background due to the transducer and bonds. As can be seen from the figure, in the normal state, attenuation decreases monotonically with temperature for all applied field values in this experiment. The fact that all cooling

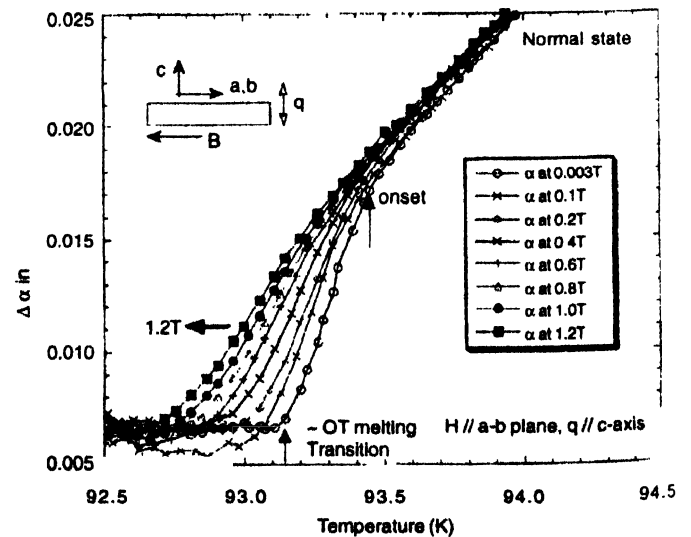


Figure 2. Attenuation vs temperature at different magnetic fields applied parallel to a-b plane of the crystal.

curves in the normal state fall exactly on each other is expected. Normal state electronic properties are not effected by fields (at least in the field range that this work was performed). This also corroborates a basic claim that if the coupling between the sample and transducer is just optimal, any effect seen in the superconducting state *i.e.* below the critical temperature, is solely due to dissipation in the superconducting state.

As the sample is cooled below the critical temperature, attenuation starts to drop faster. For actual calculations, the deviation from the linear part is taken as the onset point. As an aid, the onset of the drop at  $\sim 93.5\text{K}$ , for  $B = 0.0035\text{T}$  is approximately marked with an arrow. Decrease of attenuation is viewed as equivalent to less loss in the system, while an increase is viewed as more loss. While passing from normal to the superconducting state, the crystal goes to a more ordered state and hence there is less acoustic energy dissipation via scattering in the system. Hence it can be argued that this onset of the drop in attenuation represents onset of transition from normal to superconducting state. On the other hand, below the transition temperature, flux lines are present in the superconductor in an entangled "liquid" form and their thermal and sound induced motion becomes important. Thus at subsequently higher fields, attenuation (dissipation) is also higher (at same temperature). A plot of the applied field *vs.* onset temperature is shown in Figure 3. The solid line is a fit leading to temperature dependence of  $B$  as  $B \propto (1-t^2)$  where  $t$  is the reduced temperature  $t = T/T_c$ . The best fit is generated without using the data point at  $0.0035\text{T}$ . It is interesting to note that the mean field expression for  $H_{C2}$  also has the same  $(1-t^2)$  dependence. The resulting  $T_c(0)$  from that fit is  $\sim 93.47\text{K}$  which is just the right critical temperature at zero field when thermal lag is accounted for. The slope of the fitted curve at  $T_c(0)$  (taken as  $93.47\text{K}$ ) is  $\sim 5.6\text{T/K}$ . The upper critical

field value of  $261\text{T}$  and the slope at  $T_c$  agrees well with some published [4] numbers. Hence, it can be safely concluded that the onset of this step-like drop in attenuation marks the normal to superconducting transition point.

Figure 3 also shows a plot of endpoints of the transition at different fields. The endpoint is chosen to be the point where the attenuation values for different fields levels off. These points are approximately marked with arrows in Figure 2. Simple curve fitting resulted in a field dependence as  $B \propto (1-t)^2$  which is quite different from one found before. This  $B_m(t) \propto (1-t)^2$  dependence perfectly matches the theoretical expression for melting or freezing field for the flux line lattice. Flux lattice melting is a transition from a randomly oriented and entangled liquid state of the flux lines to a more ordered solid state where they are arranged in a regular manner. The motion of flux lines is impeded by coupling of the flux lines with the ionic background of the crystal. This motion or source of dissipation vanishes as the sample temperature reaches a value where the flux lines "freezes" in a presumably regular array forming a solid flux lattice.

#### 4. Conclusions

The results point to the fact that under optimal experimental conditions, sampled CW is not limited to probing the HTSC samples only when the flux lines are pinned or nearly pinned but rather can probe a large temperature and field range where the interaction mechanism is different. All earlier results on sintered HTSC material and using pulse-echo type of measurements revealed only the broad relaxation peak due to TAFF (thermally activated flux flow) [5, 6]. Also earlier results on single crystals using torsional oscillator [7] and vibrating reed [8] techniques resulted in a sharp peak in dissipation, which was again identified with the depinning transition of the flux lines along with the argument that the melting phenomena follows this transition. But none of the techniques have been able to clearly separate melting transition of flux line lattice and the regime of depinning transition. These two transitions are very well separated and visible in the sampled CW results on  $\text{YBa}_2\text{Cu}_3\text{O}_{7.8}$ .

Transition from normal to superconducting state at a characteristic temperature, in near zero and non-zero magnetic field, is another major finding in this study using sampled CW technique. The results obtained for twinned YBCO are in excellent agreement with published numbers for the slope of  $H_{C2}(T)$  near  $T_c$  and the extrapolated value  $H_{C2}(0)$ .

#### Acknowledgment

This work was partly supported by National Science Foundation under grants DMR-9704020 and DMR-9971123.

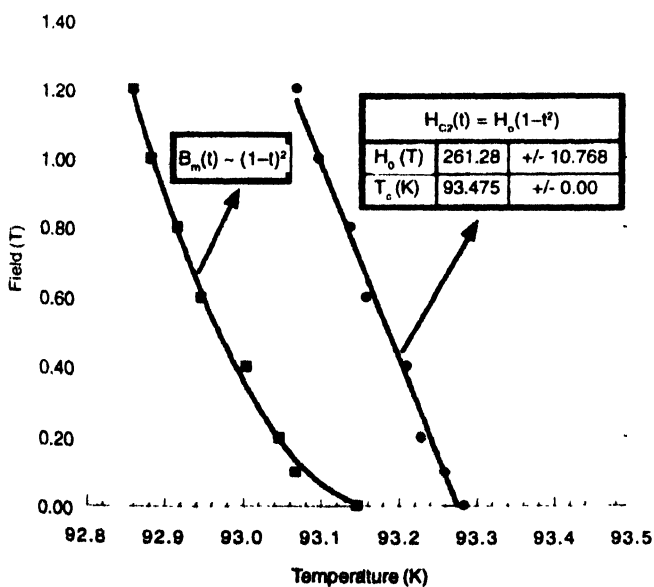


Figure 3. Field *vs.*  $T^*$  at the superconducting transition (right) and melting temperature  $T_m$  (left). Solid lines represent the fitted curves.

**References**

- [1] G Blatter, M V Feigel'man, V B Geshkenbein, A I Larkin and V M Vinokur *Rev. Mod. Phys.* **66** 1125 (1994)
- [2] J Pankert *Physica C* **168** 335 (1990)
- [3] J Pankert, G Marbach, A Comberg, P Lemmens, P Fröning and S Ewert *Phys. Rev. Lett.* **65** 3052 (1990)
- [4] C P Poole Jr., H A Farach and R J Creswick *Superconductivity* (San Diego : Academic) (1995)
- [5] M J Higgins, D P Goshorn, S Bhattacharya and D C Johnston *Phys. Rev.* **B40** 9393 (1989)
- [6] M Levy, M F Xu, B K Sarma and K-J Sun *Physical Acoustics* Vol. **XX** (ed) M Levy (San Diego ; Academic) (1992)
- [7] R G Beck, D E Farrel, J P Rice, D M Ginsberg and V G Kogan *Phys. Rev. Lett.* **68** 1594 (1992)
- [8] J Kober, A Gupta, P Esquinazi, H F Braun and E H Brandt *Phys. Rev. Lett.* **66** 2507 (1991)